frontiers in Earth Science

ORIGINAL RESEARCH
published: 02 August 2019
doi: 10.3389/feart.2019.00193

Mechanisms of Ash Generation at Basaltic Volcanoes: The Case of Mount Etna, Italy

Margherita Polacci[1], Daniele Andronico[2], Mattia de' Michieli Vitturi[3], Jacopo Taddeucci[4] and Antonio Cristaldi[2]*

[1] School of Earth and Environmental Sciences, University of Manchester, Manchester, United Kingdom, [2] Istituto Nazionale di Geofisica e Vulcanologia, Sezione di Catania, Osservatorio Etneo, Catania, Italy, [3] Istituto Nazionale di Geofisica e Vulcanologia, Sezione di Pisa, Pisa, Italy, [4] Istituto Nazionale di Geofisica e Vulcanologia, Sezione di Roma1, Rome, Italy

Basaltic volcanism is the most widespread volcanic activity on Earth and planetary bodies. On Earth, eruptions can impact global and regional climate, and threaten populations living in their shadow, through a combination of ash, gas and lava. Ash emissions are a very typical manifestation of basaltic activity; however, despite their frequency of occurrence, a systematic investigation of basaltic ash sources is currently incomplete. Here, we revise four cases of ash emissions at Mount Etna linked with the most common style of eruptive activity at this volcano: lava fountains (4–5 September 2007), continuous Strombolian activity transitioning to pulsing lava fountaining (24 November 2006), isolated Strombolian explosions (8 April 2010), and continuous to pulsing ash explosions (last phase of 2001 eruption). By combining observations on the eruptive style, deposit features and ash characteristics, we propose three mechanisms of ash generation based on variations in the magma mass flow rate. We then present an analysis of magma residence time within the conduit for both cylindrical and dike geometry, and find that the proportion of tachylite magma residing in the conduit is very small compared to sideromelane, in agreement with observations of ash componentry for lava fountain episodes at Mount Etna. The results of this study are relevant to classify ash emission sources and improve hazard mitigation strategies at basaltic volcanoes where the explosive activity is similar to Mount Etna.

Keywords: basaltic volcanism, ash generation mechanisms, sideromelane and tachylite, conduit magma residence time, Mount Etna

OPEN ACCESS

Edited by:
Roberto Sulpizio,
University of Bari Aldo Moro, Italy

Reviewed by:
Marco Viccaro,
University of Catania, Italy
Claudio Scarpati,
University of Naples Federico II, Italy

****Correspondence:***
Margherita Polacci
margherita.polacci@manchester.ac.uk

Specialty section:
This article was submitted to Volcanology, a section of the journal Frontiers in Earth Science

Received: *11 April 2019*
Accepted: *10 July 2019*
Published: *02 August 2019*

Citation:
Polacci M, Andronico D, de' Michieli Vitturi M, Taddeucci J and Cristaldi A (2019) Mechanisms of Ash Generation at Basaltic Volcanoes: The Case of Mount Etna, Italy. Front. Earth Sci. 7:193. doi: 10.3389/feart.2019.00193

INTRODUCTION

Explosive volcanism is characterised by magma fragmenting into particles of different size varying from micrometre to metre. In the presence of an eruption column, ash particles are volcanic fragments up to 2 mm in size that are dispersed to large distances from the eruptive centre in comparison to coarser fragments (e.g., bombs and lapilli) that fall in more proximal areas. Abundant ash has characterised most of the explosive activity at Mount Etna, Italy, since 1995 (**Figure 1**) (e.g., La Delfa et al., 2001; Alparone et al., 2003; Andronico et al., 2009a, 2015 and references therein), often deeply affecting people's everyday life and the overall economy of Eastern Sicily (e.g., Barsotti et al., 2010; Andronico et al., 2014a; Andronico and Del Carlo, 2016; Horwell et al., 2017).

FIGURE 1 | Satellite images of ash dispersal during the 2001 and 2002–2003 Mount Etna eruptions. **(a)** July 22, 2001; Image courtesy Jacques Descloitres, MODIS Land Rapid Response Team at https://visibleearth.nasa.gov/view.php?id=56431. **(b)** October 27, 2002; image courtesy Jacques Descloitres, MODIS Rapid Response Team at NASA GSFC, at https://visibleearth.nasa.gov/view.php?id=10376. **(c)** November 12, 2002; image courtesy Jeff Schmaltz, MODIS Rapid Response Team, NASA GSFC at https://visibleearth.nasa.gov/view.php?id=10398. Mount Etna coordinates 37°45′18″N, 14°59′42″E.

At Etna ash emissions accompany different eruptive styles, from mild to moderate Strombolian explosions to high energy lava fountain activity (e.g., Andronico et al., 2008a, 2015), from short-lasting ash explosions (Andronico et al., 2013) to long-lasting explosive eruptions like those occurred in 2001 (20 days; e.g., Taddeucci et al., 2002; Scollo et al., 2007) and in 2002–2003 (∼2 months; e.g., Andronico et al., 2005). All the 1995–2019 explosive activity producing significant ash emissions in the atmosphere and involving summit craters or flank areas has been summarised in **Table 1**.

Based on visual observations of the eruptive activity and textural and compositional features of ash samples, it was found that the characteristics of ash particles at Etna usually vary with the eruptive style. For example, ash emitted during Strombolian explosions and at the peak of lava fountain activity is more vesicular, less crystallised and with a less compositionally evolved groundmass than that erupted during less explosive events or at the end of a long-lasting explosive eruption, and it contains less lithic material (Taddeucci et al., 2004; Andronico et al., 2008b). Based on ground and satellite data, Andronico et al. (2009b) have attempted a first classification of ash-enriched Etnean volcanic plumes, subdividing ash emissions in the autumn of 2006 into five categories and demonstrating the utility of such classifications for volcanic hazard mitigation planners and civil protection purposes. It is worth specifying, however, that this classification is valid mostly for that period of activity in 2006 and it does not cover the whole range of explosive activity displayed by Etna.

Previous research on ash characteristics and the link between ash and eruption behaviour has improved our general knowledge on ash emissions at Etna (Taddeucci et al., 2002; Andronico et al., 2013). A better understanding of ash formation has the potential of further improving hazard assessment and forecasting at this volcano. However, while the sources and features of ash particles at Etna have been investigated in several cases, a systematic comparison is still lacking. The present paper represents a concrete step forward in the attempt of classifying the most common mechanisms through which ash originates at Etna. In the following, first we briefly revise the characteristics of Etna ash, then we present four different case studies of ash emissions, each associated with a different eruptive style and marked by a different duration and intensity (i.e., mass eruption rate; MER) of the tephra emission. Ultimately, we link each ash emission case study to a different, peculiar mechanism of ash formation. Although based on case studies from Etna, the proposed mechanisms can explain ash generated by other basaltic volcanic systems [e.g., Paricutin, Mexico (Pioli et al., 2008), and Villarrica, Chile (Romero et al., 2018)] which, during specific eruptive phases, resemble closely the Etna explosive activity in terms of duration, intensity and style of emission.

CHARACTERISTICS OF ASH AT ETNA

Textural and compositional features of ash particles erupted from explosive activity at Etna have been described in previous studies, and for details on the topic the reader is referred to those works (e.g., Taddeucci et al., 2002, 2004; Andronico et al., 2009a, 2013, 2014b). Here we summarise the common aspects that can help extending from specific to general cases. Juvenile ash particles at Etna consist of two end-members: sideromelane and tachylite (**Figure 2**). The former has fluidal to irregular morphology, is yellow to brown in colour, transparent, vesicular and generally glassy in the groundmass. The latter is blocky, grey to black, generally opaque (sometimes it can be shiny), poorly vesicular and crystallised in the groundmass. There is however, a continuous, progressive transition of textural features between the two ash types, mainly generated by the different extent of groundmass crystallisation, far more pronounced in tachylite, and by the higher content of (sub) spherical vesicles, as opposed to vesicles with complex and/or irregular shapes, in sideromelane (**Figure 2**). As a general rule, glass composition of Etna ash overlaps with the compositional field of pyroclastic material erupted from this volcano since 1995 (Corsaro et al., 2017; Pompilio et al., 2017). Within the same eruption, tachylite glass tends to be more compositionally differentiated in comparison to its sideromelane counterpart, with a higher silica, alkali and phosphorous content and lower magnesium and calcium (Taddeucci et al., 2002, 2004; Polacci et al., 2006). Compositional variations are mainly related to fractionation of a few tens of percent of crystal phases forming the groundmass. Lithic

TABLE 1 | Summary of the explosive activity (summit eruptions, i.e., lava fountains, strong Strombolian episodes, Strombolian explosions and sustained ash emissions, and flank eruptions) producing significant ash emission up to tens–hundreds of kilometres of distance away from Etna from 1995 to 2017.

Date	NEC	VOR	BN	SEC	NSEC	Flank activity	References
November 9, 1995–June 25, 1996	10 lava fountains						Coltelli et al., 1998, 2000
March 27, 1998		Lava fountain					La Delfa et al., 2001
July 22 and August 6, 1998		2 lava fountains					La Delfa et al., 2001
September 15, 1998–February 4, 1999			22 lava fountains				La Delfa et al., 2001
September 4, 1999		Lava fountain		Lava fountain			Cannata et al., 2008
Ocotber 17–November 3, 1999			10 Strong Strombolian episodes				Harris and Neri, 2002
January 26–June 24, 2000			64 lava fountains				Alparone et al., 2003
May 9, 2001				Strong Strombolian episode			La Spina et al., 2015
June 7–July 17, 2001			15 lava fountains				La Spina et al., 2015
July 17–31, 2001						S flank	Taddeucci et al., 2002; Scollo et al., 2007
October 27–December 30, 2002						S and NE flanks	Andronico et al., 2005 Andronico et al., 2008a
August 30–November 27, 2006				18 Strong Strombolian episodes			Andronico et al., 2009a
November 27–December 15, 2006				Ash emission episodes			Andronico et al., 2009b
March 29–November 23, 2007				5 lava fountains 1 Strong Strombolian episode			Andronico et al., 2008a Acocella et al., 2016
May 10, 2008				Lava fountain			Bonaccorso et al., 2011
April 8, 2010				Strombolian explosion			Andronico et al., 2013
August 25, 2010			Strombolian explosion				Andronico et al., 2013
December 22, 2010			Strombolian explosion				Andronico et al., 2013

(Continued)

TABLE 1 | Continued

Date	NEC	VOR	BN	SEC	NSEC	Flank activity	References
January 11, 2011–April 24, 2012				25 lava fountains			Behncke et al., 2014
February 19–April 27, 2013				13 lava fountains			Poret et al., 2018b; De Beni et al., 2015
October 25–December 26, 2013					6 lava fountains		De Beni et al., 2015
December 15 and 30, 2013				2 Strombolian episodes			Poret et al., 2018a; De Beni et al., 2015
December 3–5, 2015		4 lava fountains					Corsaro et al., 2017
May 18–21, 2016		3 lava fountains					Edwards et al., 2018
March 15–18, 2017							Andronico et al., 2017
24 December 2018	Strong Strombolian activity		Strong Strombolian activity			E flank of Etna	Neri, 2018
January–February 2019	Several episodes of pulsating to continuous ash						Andronico, pers. comm; Behncke and Neri, 2019

NEC, North-East Crater; VOR, Voragine; BN, Bocca Nuova; SEC, South-East Crater; NSEC, New South-East Crater.

FIGURE 2 | Secondary (top) and backscattered (bottom) scanning electron microscope images of typical sideromelane **(a,c)** and tachylite **(b,d)** ash particles at Mount Etna. Scale bar 20 μm in all images.

ash from Etna eruptions is not always easily distinguishable from tachylite juveniles, but is often marked by altered/oxidised surfaces and secondary minerals overgrowths.

Visual observations of the eruptive activity integrated with investigations of ash componentry have revealed that the proportion of sideromelane ash increases with increasing eruption intensity (Taddeucci et al., 2004, and this work, section "Representative Episodes of Ash Emission at Etna"). Therefore, Strombolian and lava fountain activity generally produce more sideromelane and fewer tachylite than low energy, impulsive ash explosions (Andronico et al., 2008b). This correlation, together with textural and compositional observations, suggested a longer conduit residence time for tachylite with respect to sideromelane ash. Hence, several authors hypothesised that tachylite ash particles at Etna are generated by the fragmentation of a cooler, viscous, crystallised and degassed magma at the conduit walls, while sideromelane represents the hotter, less viscous and vesiculating magma rising in the central portion of the conduit (Taddeucci et al., 2004; Polacci et al., 2006; Pompilio et al., 2017).

Ash dispersal at Etna is mostly controlled by eruption intensity and the ensuing plume height, as expected. For example, on 23 February and 23 November 2013, two lava fountain episodes characterised by relatively high eruption columns (at least for the most common explosive activity at Etna) of up to 9–10 km a.s.l. and high MERs, generated dispersal of ash particles up to 400 km from Etna, in Puglia (Italy) (Poret et al., 2018a,b). Lower intensity impulsive explosions and discontinuous explosive activity generally produce lower and intermittent eruption columns above the vent, producing minor ash dispersal. However, if the intensity is low but the duration of the activity is prolonged for days to weeks, the continuous injection of relatively fine-grained ash in the atmosphere is able to form a sustained tephra column feeding an eruption cloud spreading hundreds of km away from the volcano. This occurred, for example, during the 2001 and 2002–2003 eruptions

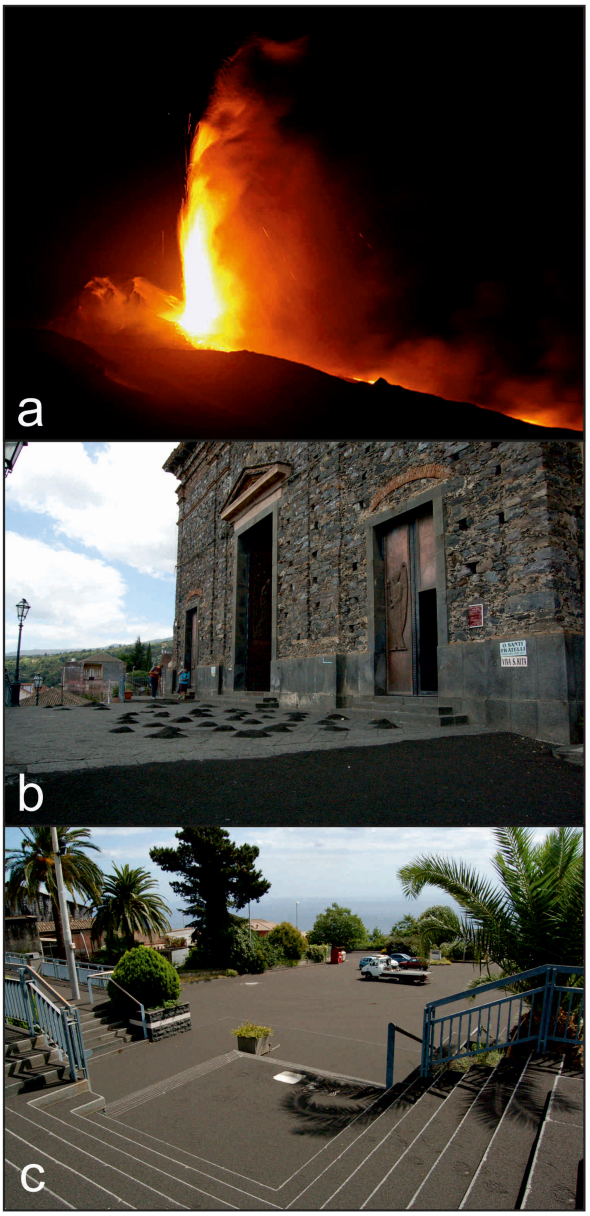

FIGURE 3 | 4–5 September 2007 lava fountain at Mount Etna: **(a)** magma jets from the South-East Crater (photo at https://forum.meteonetwork.it/meteo-foto/62785-eruzione-etna-04-settembre-2007-a.html); **(b,c)** images of the tephra deposit in the village of S. Alfio, ∼13 km from the vent (photo by Daniele Andronico). Reproduced with permission.

(e.g., Andronico et al., 2005; Villani et al., 2006; Scollo et al., 2007) (**Figure 1**).

REPRESENTATIVE EPISODES OF ASH EMISSION AT ETNA

In the following we present and revise four case studies, in order of decreasing eruption intensity, during which ash was vented at Etna from either a single, short-lasting (minutes to tens of hours) explosive event (i.e., 24 November 2006, 4–5 September 2007, 8 April 2010) or a longer period of erupted activity that involved several successive explosive events over the course of a week (i.e., the last phase of the 2001 eruption). We have chosen these specific case studies because they cover the most common eruptive styles and intensities that have characterised the explosive activity at Etna in the last decades: sustained lava fountain activity (the 2007 event), continuous Strombolian activity transitioning to quasi-steady or pulsing lava fountain (the 2006 event), isolated Strombolian explosions (the 2010 event) and nearly continuous to pulsing ash explosions (the 2001 eruption). For each case study we provide a brief description of the event (or eruption), as well as a description of the associated deposit and ash particle features. This overall information represents a basic framework for classifying ash emissions at Etna and provides the constraints necessary to model mechanisms of ash formation.

Case Study No. 1: The 4–5 September 2007 Sustained Lava Fountain

This episode of lava fountain from the Southeast Crater (SEC) at Etna is one of the best studied lava fountains occurred in the last 40 years of eruptive history of the volcano for its long duration (about 10 h) and steady, sustained, violent jets of magma and gas resulting in a continuous 2 km-high eruption plume (Andronico et al., 2008a) (**Figure 3**). For the high eruptive intensity and the textural features of the erupted ejecta, this activity compares well with the most energetic episodes of the well-studied paroxysmal, cyclic fountaining activity that characterised SEC in 2000 (Alparone et al., 2003; Polacci et al., 2006) and the New Southeast Crater (NSEC) in 2011–2012 and 2013 (e.g., Behncke et al., 2014; De Beni et al., 2015). The paroxysmal sequences at NSEC, in particular, included also very high energy episodes characterised by high eruption columns (7–8 km above the vent; Scollo et al., 2014) and very large spreading of tephra up to 400 km from the vent (e.g., Poret et al., 2018a,b). This suggests that the magnitude of lava fountains at Etna may range significantly, in terms of eruption column height and MER, from small- to large-scale events (Andronico et al., 2015). This terminology also well describes the four lava fountains episodes which took place in December 2015 at the Voragine crater. These episodes were, in fact, characterised by large-scale eruption columns, reaching the troposphere-stratosphere boundary and forming relatively thick tephra deposits on the volcanic slopes (Vulpiani et al., 2016; Corsaro et al., 2017; Pompilio et al., 2017; Cannata et al., 2018). The tephra deposit (**Figures 3B,C**), resulting from the juvenile material fallout from the Eastward directed plume of the 4–5 September lava fountain, blanketed an area on the mainland extending up to 19 km away from the vent before being subsequently dispersed in the Ionian sea (Andronico et al., 2008a). Investigations carried out on the ash collected in medial and distal areas reveal that the whole sample is completely made up of sideromelane particles containing large sub-spherical vesicles, with a minor proportion of sideromelane

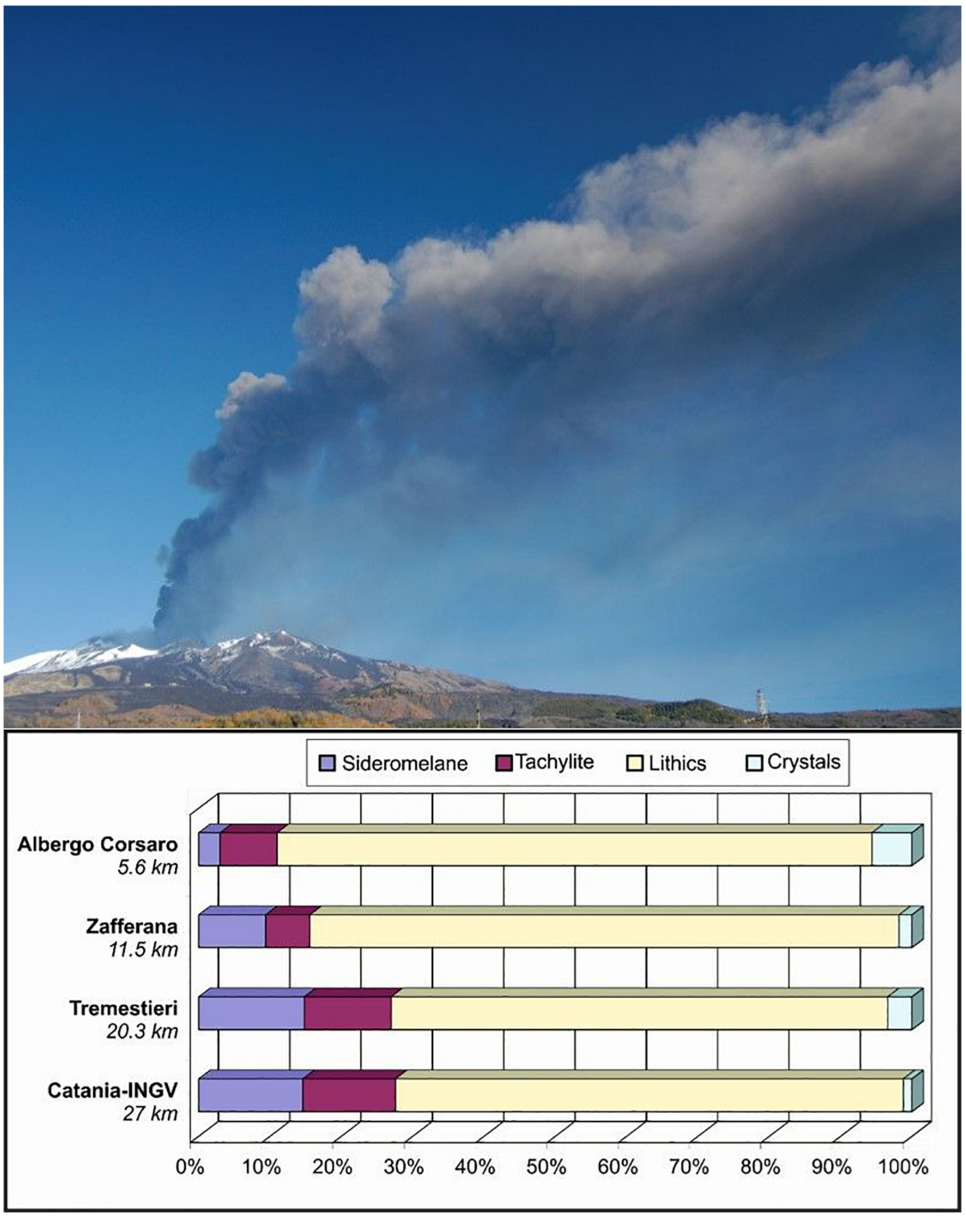

FIGURE 4 | Plume of the 24 November 2006 activity (from Polacci et al., 2009) and diagrams illustrating the relative abundance of ash componentry at different distances from the vent. Reproduced with permission.

particles characterised by a high number of smaller vesicles (Andronico et al., 2008a).

Case Study No. 2: The 24 November 2006 Continuous Strombolian Activity

The explosive activity that occurred at SEC on 24 November 2006 represents one of the paroxysmal episodes that took place at Etna during the August–December 2006 eruption. Such explosive activity developed high energy, continuous Strombolian explosions that transitioned to a quasi-sustained or pulsing lava fountain for about 13 h generating an ash plume up to 2 km high on the summit craters and rotating from SE to S (De Beni et al., 2006; Nicotra and Viccaro, 2012; Andronico et al., 2014b) (**Figure 4**). Based on their steady supply, duration and large tephra fallout, Andronico et al. (2009b) classified plumes like the one generated by the 24 November 2006 explosive activity as *middle eruptive intensity plumes*, the most dangerous plume type, in terms of volcanic hazard, throughout the 2006 autumn Etna eruption. Long, though small-scale, eruptions lasting several hours like the 24 November 2006 event may cause greater anxiety and worry to the local population and authorities than shorter and higher intensity eruptions (e.g., 12 January 2011; Andronico et al., 2014a). Indeed, the relatively

low eruption intensity, combined with the long-lasting tephra fallout, was enough to produce a continuous deposit up to distances of 15 km from SEC. At greater distances (∼25–30 km), a discontinuous tephra layer formed in the city of Catania and surroundings (**Figure 4**) where, although at a low sedimentation rate on the ground (5–6 g/m^2 h^{-1}; Andronico et al., 2009b, 2014b), the ash dispersal caused temporary closure of the airport infrastructures and disruption to the air traffic. During this activity, the emitted ash was composed mostly of lithic particles (typically subrounded and with weathered surfaces), while the juvenile fraction (sideromelane and tachylite) represented about a quarter or less of the ash componentry in most of the collected samples at different distances from the vent (Andronico et al., 2014b). Tachylite fragments were microcrystalline, blocky and characterised by fresh, angular surfaces, while sideromelane clasts were mainly glassy with irregular to elongate shape. Hybrid partially crystallised particles made of both sideromelane and tachylite were also present (Andronico et al., 2014b).

Case Study No. 3: The 8 April 2010 Single Strombolian Explosion

This case study is well representative of the explosive activity occurred in 2010, when the Etna summit craters produced several single or short sequences of impulsive ash release events, lasting usually less than 1 min. Most of them consisted of small failures involving the rims and/or the inner walls of the summit craters; however, some of them were much more intense and correlated with seismic and acoustic signals (Andronico et al., 2013), suggesting some magmatic dynamics were involved in it. One of the major explosions took place on 8 April 2010 at SEC and produced a dark ash emission rising quickly up to 600–700 m of height above the eruptive vent, which formed a small eruption cloud dispersed to the NE (Andronico et al., 2013) (**Figure 5**). Light tephra fallout occurred at Linguaglossa, a village located 16 km from the vent, where the ash deposit had unimodal grain-size distribution (peaked at 0.25 mm) and a mass loading of 18 g/m^2 (Andronico et al., 2013).

Another example of this activity is the ash emission that rose a few hundred metres above SEC on 29 October 2006, forming a diluted ash plume which generated modest tephra fallout on the southern slopes of the volcano. A thin, discontinuous ash layer was deposited up to Catania, reaching a maximum loading of 30 g/m^2 at Rifugio Sapienza (∼5 km from the vent) and a minimum of 5 g/m^2 in Catania (∼27 km from the vent) (Cristaldi and Scollo, 2006). Lithic clasts dominated the ash componentry in both cases. On 8 April, furthermore, between 4.7 and 16 km from the vent, the ash consisted mainly of tachylite (12–27%), a variable, decreasing fraction of sideromelane particles (from 18 to 1%), abundant lithics including weathered volcanic fragments of glass and crystals (∼50–80%), and negligible amounts of crystals (2–5%) (**Figure 5**). On 29 October the distal erupted ash mainly consisted of lithics (56%) and tachylite (34%) particles, with poor or negligible percentages of sideromelane (8%) and crystals (2%), respectively (**Figure 5**) (Cristaldi and Scollo, 2006).

Case Study No. 4: The Ash Explosions During the Last Phase of the 2001 Eruption

In comparison to case studies 1, 2, and 3, where the eruptive activity involved one of the summit craters, the July–August 2001 Etna eruption was marked by lateral activity and the ash was emitted mostly by two newly-formed vents located at 2550 and 2100 m a.s.l. on the south flank of the volcano. In the last phase of the July–August 2001 Etna eruption (1–7 August 2001), the activity at the 2550 m a.s.l. vent transitioned from spatter-forming Strombolian explosions to a series of sustained to pulsed, ash-rich explosions (Taddeucci et al., 2002, 2004). Ash erupted at first as an almost continuous plume; then the intensity and frequency of explosions decreased to isolated, cannon-like events producing discrete plumes. Plumes were easily bent by moderate wind and their height was in the 500–1500 m range. Ash from these plumes was deposited very locally, reaching a total thickness of about 20 cm at a distance of about 50 m eastward of the vent (Taddeucci et al., 2002). Ash deposited in this time window presents a gradual but systematic increase (from about 64 to 73 particles %) of blocky, poorly vesicular to non-vesicular, microlite-rich tachylite particles at the expenses of sideromelane, and a small increase (from 1 to 7%) of lithic particles. These changes are accompanied by a concomitant decrease in the overall vesicularity of the ash particles (Taddeucci et al., 2002) (**Figure 6**).

DISCUSSION

Mechanisms of Ash Formation at Etna

We present here three mechanisms of ash formation that we link with the four different types of ash emission activity described in the previous section. We anticipate however, that such mechanisms may not be exhaustive to describe and explain mechanisms of ash formation at Etna or other basaltic volcanoes characterised by ash emission activity, and that other mechanisms may therefore be feasible. We propose that variations in the magma mass flow rate are a common, key-parameter in determining variations in the style of activity of erupted ash, translating into different mechanisms of ash generation.

Mechanism No. 1 (The Sustained 4–5 September 2007 Lava Fountain and the Continuous Strombolian Activity of 24 November 2006)

The first mechanism concerns ash accompanying lava fountain activity and generated by fragmentation of fast-rising (order of 10 to 40 m/s, La Spina et al., 2016; Giuffrida et al., 2018), vesiculating magma. Previous studies have well documented that lava fountaining from SEC at Etna is driven by the superposition of two distinct outgassing mechanisms, gas foam collapse and syn-eruptive vesiculation in the glassy pockets between bubble walls (**Figure 7**) (Allard et al., 2005; Polacci et al., 2006, 2009; Vergniolle and Ripepe, 2008). Drawing from the model of Jaupart and Vergniolle (1988, 1989), we assume here that gas bubbles are exsolved and accumulated in a foam layer at the roof of a storage area below the eruptive crater (**Figure 7**). We also assume

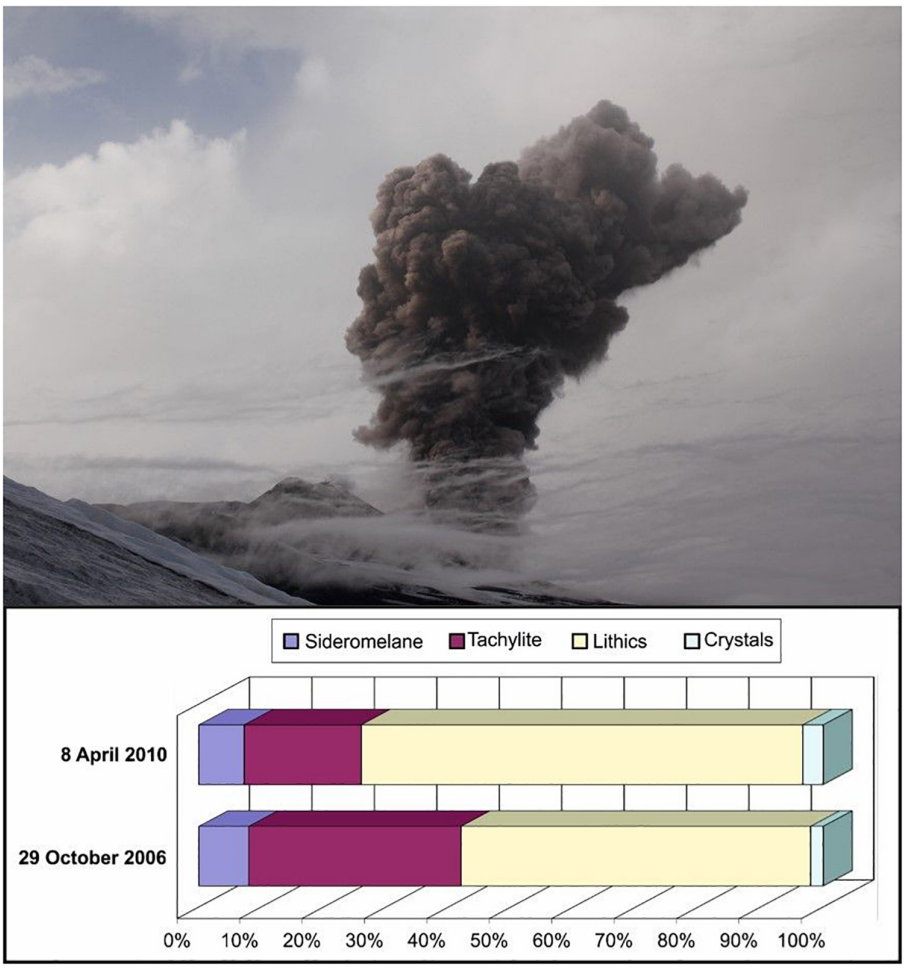

FIGURE 5 | Image of the peak in activity of the 8 April 2010 explosion and comparison between the ash componentry of the 29 October 2006 explosion and the average value of 4 samples collected at increasing distance from the vent after the 8 April 2010 explosion (data Andronico et al., 2013). Photo from Thomas Bretscher at https://www.flickr.com/photos/bretscher/4508419186/in/album-72157623824783982/. Reproduced with permission.

that an increase in the magma mass flow rate into the storage area increases the bubble supply to the foam, promoting bubble coalescence and enhancing the potential for the foam layer to collapse, ascend rapidly and fragment explosively at the top of a magma column that fills the conduit almost entirely. Considering a storage area depth of approximately 1.5–1.9 km (at least for SEC; Bonaccorso, 2006), the rapidity and intensity with which the fountain events take place do not allow the involved magma to reside in the conduit for longer than a few minutes (see section "Analysis of magma residence time in conduits"). This greatly limits the occurrence of magma cooling and crystallisation at the conduit walls, and, as a result, decreases the generation of tachylite and its presence in the deposited ash. We suggest that the combination of the two outgassing mechanisms described above, foam collapse and syn-eruptive vesiculation, results into a more efficient and rapid magma fragmentation, providing a constant supply of vesicular sideromelane ash to the erupted plume. These observations agree with the characteristics of the sideromelane ash produced by the lava fountain episode of the 4–5 September 2007 (see section "Representative Episodes of Ash Emission at Etna").

Tachylite ash was present in the ash samples collected after the continuous Strombolian activity that transitioned to pulsating lava fountain activity of the 24 November 2006. This episode was subdivided into three main eruption phases (resumption, paroxysmal and conclusive), similarly to what was proposed for the 2000 lava fountains by Alparone et al. (2003). It started with high energy Strombolian explosions that increased in frequency and intensity with time originating a quasi-sustained lava fountain, where the pulsed behaviour may be explained in terms of oscillations in the magma mass flow rate, hence, in the bubble supply rate to the foam layer. Sustained lava fountaining lasts as long as the bubble supply is sufficient to sustain the critical thickness needed for the foam layer to collapse. If the bubble supply rate decreases, the foam layer critical thickness may be no longer supported and the steady fountain phase of the event ceases, progressively shifting to pulsed behaviour and/or less energetic Strombolian explosions

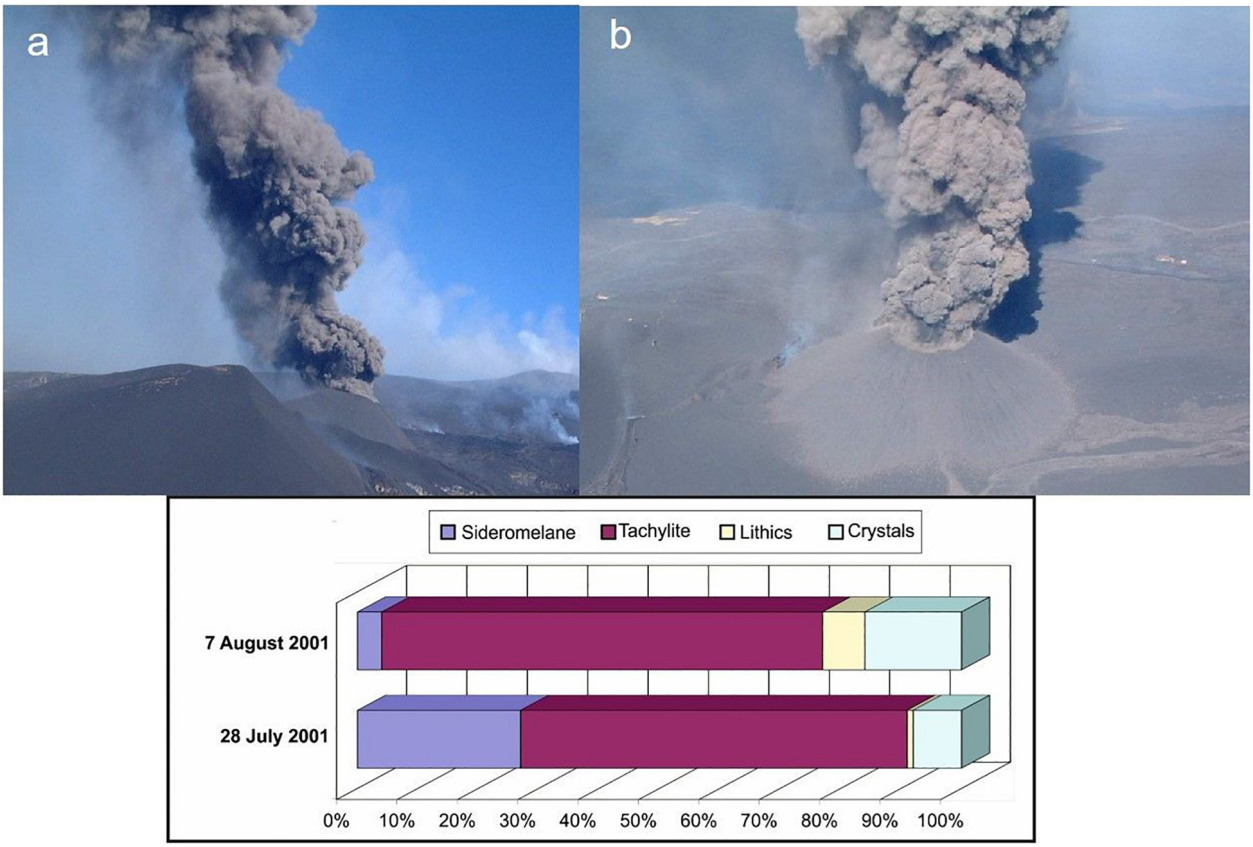

FIGURE 6 | Images **(a,b)** of the pulsing ash plume generated during the final phase of activity of the vent at 2550 m a.s.l. in 2001, and diagrams of ash componentry at the beginning and at the end of this final phase of activity. Reproduced with permission.

till, eventually, the end of the activity. Potential consequences deriving from this series of events are sudden changes in the magma fragmentation depth, longer magma residence time in the conduit, increasing proportion of cooled, crystallised (tachylite-like) magma vs. vesiculating (sideromelane-like) magma, and variations in the proportion of sideromelane vs. tachylite ash particles in the deposited fragmented magma (section "Analysis of magma residence time in conduits"). Ultimately, the pressure decrease associated with the lack of a sustained magma column inside the conduit, occurring during the initial and waning phase of an eruption, can favour the collapse of conduit walls and the production of lithics (Aravena et al., 2018). Similarly, pressure profiles associated with smaller conduits favour conduit walls instability and thus eruptions with a higher proportion of lithic fragments (Aravena et al., 2017). This explains the high abundance of lithics in the ash componentry of the 24 November 2006 activity (see **Figure 4**).

Mechanism No. 2 (The Last Phase of the 2001 Eruption)

The second mechanism concerns ash produced by low energy explosive activity or by impulsive explosions that characterise the final period of a prolonged explosive eruption. This type of ash is generated by the fragmentation of a partially degassed magma column occupying the conduit and left from previous explosive activity. We envisage that slugs or pockets of gas rise across the magma and burst at the free magma surface progressively emptying a magma body that is increasingly cooler, crystallising and losing gas both vertically and horizontally from the conduit centre to the walls (**Figure 8**). Here vesicles are deformed and collapsed by both magma strain rate and increasing crystallisation, eventually generating the complex vesicle shapes typical of tachylite-forming magma (Taddeucci et al., 2004; Polacci et al., 2006). This mechanism of ash formation from a tachylite-rich magma well agrees with descriptions of the dynamics and tephra samples characterising the last phase of the 2001 Etna eruption. During this period of explosive activity, a decrease in the magma mass flow rate determined also a decrease in the eruption explosivity (Taddeucci et al., 2004), allowing a proportion of magma to stagnate in the proximity of the conduit walls and promoting an increase of tachylite versus sideromelane ash in the related deposited fragmented magma (**Figure 8** and section "Analysis of magma residence time in conduits"). In comparison to the first mechanism, the ash fallout generated by mechanism no. 2 is fewer because the explosive events from which it is erupted are shorter in duration and significantly less energetic than lava fountain activity. In addition, the ash is finer than that erupted from a lava fountain because

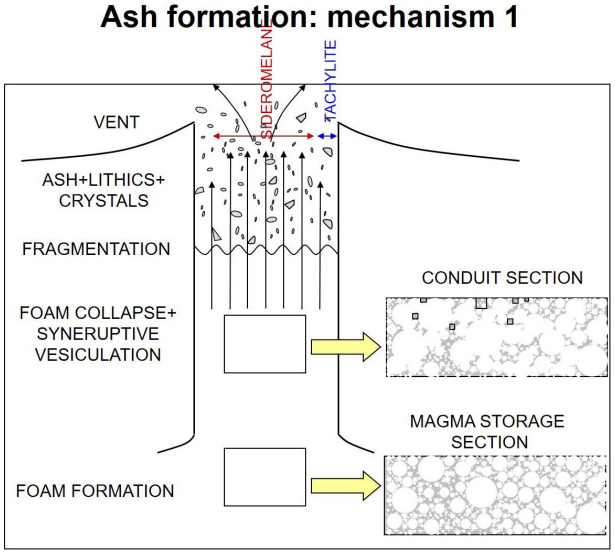

FIGURE 7 | Sketch of ash formation by fragmentation of vesiculating magma (mechanism no. 1). Grey areas in conduit section and in magma storage section insets indicate liquid magma (plus crystals). Not to scale. See text for further explanation.

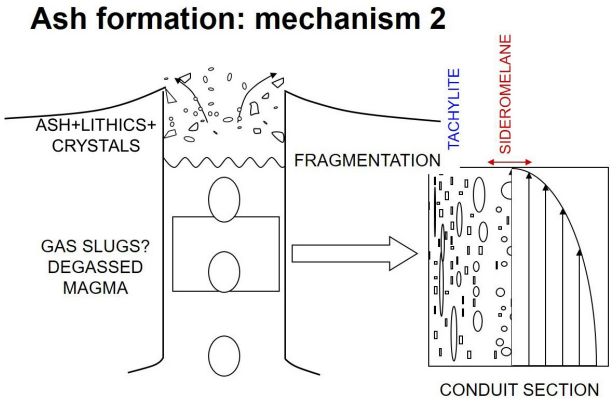

FIGURE 8 | Sketch of ash formation by fragmentation of partially degassed magma (mechanism no. 2). In conduit section inset arrows indicate increasing velocity gradient from conduit centre (where sideromelane is) to walls (where tachylite is). Not to scale. See text for further explanation.

this mechanism of formation involves, besides ash from primary magmatic fragmentation, material eroded from the conduit walls and/or collapsed inside the crater, as well as recycled ash particles (e.g., ash particles that have been ejected and that fall back into the conduit; D'Oriano et al., 2014). This is supported by comparing grain-size data from the 4–5 September 2007 lava fountain (Andronico et al., 2008a) and 24 November 2006 pulsed lava fountain (Andronico et al., 2014b) with those from distal samples of the last phase of the 2001 eruption: the latter has a mode at 2.5–3 phi (Cristaldi and Andronico, pers. comm.), while the former have a coarser mode considering the grain-size distribution of both the total deposit and single samples collected at comparable

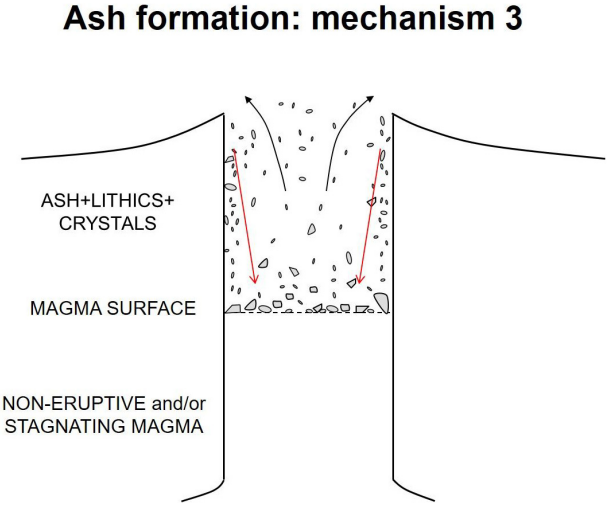

FIGURE 9 | Sketch of ash formation by collapses of intracrateric material and conduit lining (mechanism no. 3). Red arrows indicate collapsing material. Not to scale. See text for further explanation.

distances. Given these particles were generated during a flank eruption, the different shallow feeding system may have affected ash generation and, consequently, componentry, changing for example the proportion of tachylite versus sideromelane with respect to the case where ash is vented from a central vent/crater along a well, already structured and relatively wider conduit.

Mechanism No. 3 (The 8 April 2010 Single Strombolian Explosion)

The third mechanism highlighted in this study mainly concerns ash produced by collapses of intracrateric material and conduit lining (**Figure 9**). Visual observations and images from video cameras as well as seismic and infrasonic signals suggest that this mechanism of ash formation is often promoted by intracrateric gas jets or isolated Strombolian bursts. Such mechanism usually occurs at the end of a high energy Strombolian explosive episode or between consecutive explosive events within an eruption or within a period of explosive activity, the latter case being nicely illustrated by the April 8 2010 explosion (Andronico et al., 2013). In agreement with features displayed by ash erupted from this episode and from the 29 October 2006 event, ash generated by mechanism no. 3 mainly consists of lithic particles (weathered scoria and lava fragments from the conduit walls) and microlite-rich tachylite ash from the cooling, crystallising magma skin at the conduit walls and the very top of the magma column filling the conduit. Notwithstanding the prevalence of lithic clasts in the ash componentry during ash emissions in 2010, the presence of clear seismic and acoustic geophysical signals may help to detect the presence of a pressurised magma/gas trigger and thus to hypothesise the possible involvement not only of old and/or stagnating magma but also of fresh material (Andronico et al., 2013). This mechanism is similar to type 2 Strombolian activity described for Stromboli volcano by Patrick et al. (2007).

Analysis of Magma Residence Time in Conduits

Processes occurring in volcanic conduits, the pathways through which magma travels from its storage region to the surface, have a fundamental control on the nature of eruptions and associated phenomena (Polacci et al., 2017). In the previous sections we have seen how the relative amount of tachylite and sideromelane can be associated with different residence times of magma within the conduit, and thus with different ascent rates that can be associated with either a different average velocity, or different ascent velocities between the centre of the conduit and the portions close to conduit walls. In this section we present an analysis, for both cylindrical conduits and dikes, aimed at quantifying the fractions of erupted mass representative of different residence times within the conduit (and thus different ascent velocities).

First of all, we introduce some notation holding for both cylindrical conduits and dikes (for further details about this analysis please refer to the **Supplementary Material**). We denote with r the distance from the axis of the conduit or the dike (see **Figure 10**), corresponding to the radius of the conduit (or the semi-width of the dike), and with u_z the vertical velocity, function of r. If $u_{z,\mathrm{avg}}$ is the average velocity, and assuming the flow being Newtonian with kinematic viscosity ν, we can introduce the Reynolds number

$$\mathrm{Re} = \frac{2\,R u_{z,\mathrm{avg}}}{\nu}$$

The Reynolds number is a dimensionless quantity allowing to predict if the flow regime is laminar (Re $<$ 2300 for a cylindrical conduit) or turbulent (Re $>$ 4000 for a cylindrical conduit). We can imagine a laminar flow as a flow where all the fluid velocity vectors line up in the direction of the flow (the vertical axis z in **Figure 10**). Below the depth of fragmentation, for typical eruptions at Etna we have $R = O\left(10^0 - 10^1\right)$, $\nu = O\left(10^{-1} - 10^0\right)$, and $u_{z,\mathrm{avg}} = O\left(10^0\right)$ (La Spina et al., 2016), and laminar flow characterises nearly the entire conduit. Thus, assuming that the flow is fully developed and introducing the normalised radius $\bar{r} = \frac{r}{R}$ and the normalised velocity $\bar{u} = \frac{u_z(r)}{u_{z,\max}}$ (where $u_{z,\max}$ is the maximum velocity), we can write:

$$\bar{u} = 1 - \bar{r}^2$$

If we denote now with $\bar{t} = \frac{t(r)}{t_{\min}}$ (where $t_{\min=1/}u_{z,\max}$ is the ascent time per unit length associated with the maximum velocity) the normalised ascent time, we can also write:

$$\bar{t} = \frac{1}{1 - \bar{r}^2}$$

It is important to observe that the two equations above are independent of viscosity, flow rate values and conduit size, and that they hold for both cylindrical and dike geometries.

Now, if Q is the volumetric flow rate through the whole cross section of the conduit, and if we denote with $Q(r)$ the cumulative volumetric flow rate through the portion from the centre up to a distance r from the axis (represented in grey in **Figure 10**), we can also introduce a non-dimensional normalised radius, defined as $\bar{Q}(r) = \frac{Q(r)}{Q}$, with $\bar{Q}(r) = 0$ for $r = 0$ and $\bar{Q}(r) = 1$ for $r = R$.

For a cylindrical conduit it holds:

$$\bar{Q}(\bar{r}) = 2\bar{r}^2 - \bar{r}^4,$$

$$\bar{Q}(\bar{u}) = 1 - \bar{u}^2,$$

$$\bar{Q}(\bar{t}) = 1 - \frac{1}{\bar{t}^2} \quad (1)$$

The last two equations allow us to quantify the volume of magma associated with different ascent velocities and with different ascent times. In particular, the last one gives, for a fixed value of $\bar{t}$, the fraction of magma residing in the conduit during the rise for a time smaller than $\bar{t}$ times the minimum ascent time.

Similarly, for a dike geometry, we have the following equation defining the normalised cumulative volumetric flow as a function of the normalised radius:

$$\bar{Q}(\bar{r}) = \frac{1}{2}\left(3\bar{r} - \bar{r}^3\right)$$

and thus, using the equations introduced above relating normalised radius, velocity and time, we obtain:

$$\bar{Q}(\bar{t}) = \frac{1}{2}\sqrt{\frac{\bar{t}-1}{\bar{t}}}\left(\frac{2\bar{t}+1}{\bar{t}}\right) \quad (2)$$

Equations (1) and (2) are independent of ascent velocity and conduit size, and thus they allow to quantify the relative proportions of volumes rising with different times also for conduits of variable width and when velocity changes during the ascent.

The two relationships between normalised cumulative volumetric flow and ascent time are plotted in **Figure 11**, where on the top axis of both the plots we have also reported a temporal

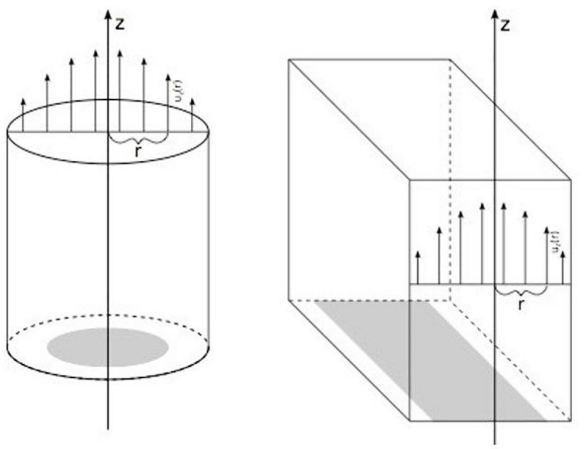

FIGURE 10 | Sketch of the geometries investigated in the analysis of conduit residence times and the velocity profiles. For both geometries, r denotes the distance from the vertical axis.

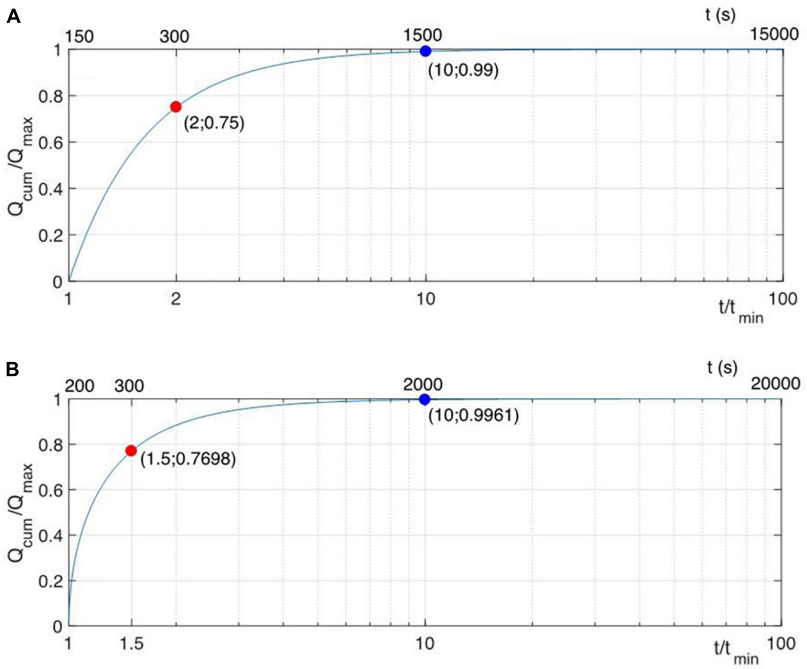

FIGURE 11 | Relationships between normalised cumulative volumetric flow and normalised ascent time for a fully-developed laminar flow in a cylindrical conduit **(A)** and in a dike **(B)**. The red dots are plotted for the average ascent time, while the blue dots for a time 10 times larger than the minimum ascent time. A non-normalised time scale is also reported on the top of each plot, where the average ascent time has been fixed to 300 s.

scale in which we assumed an average ascent time of 300 s. We remark that the average velocity for a cylindrical conduit is half the maximum velocity, while for a dike is 2/3 of the maximum velocity. Thus, for a cylindrical conduit, the fastest ascent time within the conduit (at the centre) is 150 s, while for a dike it is 200 s. The plot allows us also to quantify the portion of magma residing in the conduit for a time 10 times larger than the minimum ascent time, which correspond to 1% of the total magma for a cylindrical conduit and less than 0.4% for a dike. This is consistent with the timescales presented for mechanism 1 and the very small amount of tachylite present in the related case studies (see section "Mechanisms of Ash Formation at Etna"). In order to have a steady ascent producing a significant amount of tachylite (∼50%) at the conduit walls during the rise, it is thus needed an average ascent time one order of magnitude larger, comparable to the characteristic crystallisation times. In addition, the relationships obtained and the plots show that if the same volume of magma is erupted with the same volumetric flow rate (i.e., with same average velocity) through a dike rather than through a cylinder, the ratio between tachylite and sideromelane will be smaller. This counterintuitive result is a consequence of the higher average velocity to maximum velocity ratio of the dike with respect to the cylinder.

CONCLUSIONS

Ash emissions are widespread during explosive basaltic activity, and often have a significant impact on people's life and infrastructure. For example, between January and February 2019 Mount Etna North-East Crater produced several episodes of continuous to pulsing ash emissions, which, despite being characterised by a very low, uncommon sedimentation rate (a few g/m^2 during several hours of activity), were able nonetheless to cause disruption at the Fontanarossa International airport of Catania (29 km from the vent). To mitigate hazard at basaltic volcanoes, it is therefore imperative to improve knowledge on mechanisms of ash generation. In this study, we use Mount Etna as a general case study. Compositional and textural features of ash particles from Etna and other basaltic volcanoes have been well characterised and the explosive activity that produces them well studied. Yet, a systematic investigation of ash sources is still incomplete and mechanisms of ash generation poorly understood. With this study, we aim to fill this gap in knowledge. By revising four ash emission episodes that are representative of the most common explosive activity at Etna in the last decades, we propose three mechanisms of ash generation based on variations in the magma mass flow rate that apply to other basaltic volcanoes erupting ash and whose explosive activity is similar to Etna. Additionally, we provide an analysis of magma residence time in the volcanic conduit, which explains why different ash particles reside in the conduit for a shorter time than others. This analysis sheds light on the proportion of sideromelane and tachylite textures found in ash from lava fountaining and continuous Strombolian activity, in agreement with our first proposed ash generation mechanism. The main finding of this study is that, integrating field observations with magma residence time calculations, we are able to provide improved information

on both ash sources and mechanisms of ash formation from basaltic volcanoes erupting ash. The broader implication of this investigation is that our results are significantly relevant to the wider volcanological community, particularly modellers of eruption dynamics and scientists involved with volcano monitoring and surveillance, and should be used to improve eruption forecasting and hazard assessment and to inform stakeholders on how to implement risk mitigation strategies in active volcanic areas.

DATA AVAILABILITY

The data generated for this study are available on request to the corresponding author.

AUTHOR CONTRIBUTIONS

MP and DA conceived the study. DA, MP, and AC collated most of the literature data on the Etna activity discussed in the manuscript. JT provided data on the 2001 Etna eruption. MdMV provided the analysis of magma residence time in the conduit. MP wrote the manuscript, with contribution from all co-authors.

FUNDING

This research was funded by the RCUK NERC DisEqm project (NE/N018575/1). We also acknowledge the European Union's Horizon 2020 Research and Innovation Programme under grant agreement no. 654182, which has partially supported this research.

ACKNOWLEDGMENTS

We thank all the INGV staff at the Osservatorio Etneo in Catania devoted to the maintenance of the camera network which allows us to study the eruptive activity at Etna in great detail. We also acknowledge F. Arzilli and G. La Spina for interesting discussions on magma residence time in basaltic systems.

SUPPLEMENTARY MATERIAL

The Supplementary Material for this article can be found online at: https://www.frontiersin.org/articles/10.3389/feart.2019.00193/full#supplementary-material

REFERENCES

Acocella, V., Neri, M., Behncke, B., Bonforte, A., Del Negro, C., and Ganci, G. (2016). why does a mature volcano need new vents? the case of the New Southeast Crater at Etna. *Front. Earth Sci.* 4:67. doi: 10.3389/feart.2016.00067

Allard, P., Burton, M. R., and Mure', F. (2005). Spectroscopic evidence for a lava fountain driven by previously accumulated magmatic gas. *Nature* 433, 407–410. doi: 10.1038/nature03246

Alparone, S., Andronico, D., Lodato, L., and Sgroi, T. (2003). Relationship between tremor and volcanic activity during the Southeast Crater eruption on Mount Etna in early 2000. *J. Geophys. Res.* 108:B52241. doi: 10.1029/2002JB001866

Andronico, D., Branca, S., Calvari, S., Burton, M. R., Caltabiano, T., Corsaro, R. A., et al. (2005). A multi-disciplinary study of the 2002-03 Etna eruption: insights for a complex plumbing system. *Bull. Volcanol.* 67, 314–330. doi: 10.1007/s00445-004-0372-8

Andronico, D., Corsaro, R. A., Cristaldi, A., Lo Castro, M. D., Messina, L., Scollo, S., et al. (2017). *L'attività Esplosiva del Cratere di SE tra il 15 e il 18 Marzo 2017: Dispersione Del Deposito Distale di Caduta e Caratteristiche Tessiturali Delle Ceneri er Uttate. Rapporto Interno N. 005/2017*. Available at: http://www.ct.ingv.it (accessed May 2017).

Andronico, D., Cristaldi, A., and Scollo, S. (2008a). The 4–5 september 2007 lava fountain at South-East Crater of Mt Etna, Italy. *J. Volcanol. Geotherm. Res.* 173, 325–328. doi: 10.1016/j.jvolgeores.2008.02.004

Andronico, D., Scollo, S., Caruso, S., and Cristaldi, A. (2008b). The 2002–03 Etna explosive activity: tephra dispersal and features of the deposits. *J. Geophys. Res.* 113:B04209. doi: 10.1029/2007JB005126

Andronico, D., and Del Carlo, P. (2016). PM10 measurements in urban settlements after lava fountain episodes at Mt. Etna, Italy: pilot test to assess volcanic ash hazard to human health. *Nat. Hazards Earth Syst. Sci.* 16, 29–40. doi: 10.5194/nhess-16-29-2016

Andronico, D., Lo Castro, M. D., Sciotto, M., and Spina, L. (2013). The 2010 ash emissions at the summit craters of Mt Etna: relationship with seismo-acoustic signals. *J. Geophys. Res. Solid Earth* 118, 51–70. doi: 10.1029/2012JB009895

Andronico, D., Scollo, S., and Cristaldi, A. (2015).). Unexpected hazards from tephra fallouts at Mt Etna: the 23 november 2013 lava fountain. *J. Volcanol. Geotherm. Res.* 304, 118–125. doi: 10.1016/j.jvolgeores.2015.08.007

Andronico, D., Scollo, S., Cristaldi, A., and Ferrari, F. (2009a). Monitoring ash emission episodes at Mt. Etna: the 16 november 2006 case study. *J. Volcanol. Geotherm. Res.* 180, 123–134. doi: 10.1016/j.jvolgeores.2008.10.019

Andronico, D., Spinetti, C., Cristaldi, A., and Buongiorno, M. F. (2009b). Observations of Mt. Etna volcanic ash plumes in 2006: an integrated approach from ground-based and polar satellite NOAA-AVHRR monitoring system. *J. Volcanol. Geotherm. Res.* 180, 135–147. doi: 10.1016/j.jvolgeores.2008.11.013

Andronico, D., Scollo, S., Cristaldi, A., and Lo Castro, M. D. (2014a). Representivity of incompletely sampled fall deposits in estimating eruption source parameters: a test using the 12–13 January 2011 lava fountain deposit from Mt. Etna volcano, Italy. *Bull. Volcanol.* 76:861. doi: 10.1007/s00445-014-0861-3

Andronico, D., Scollo, S., Lo Castro, M. D., Cristaldi, A., Lodato, L., and Taddeucci, J. (2014b). Eruption dynamics and tephra dispersal from the 24 november 2006 paroxysm at South-East Crater, Mt Etna, Italy. *J. Volcanol. Geotherm. Res.* 274, 78–91. doi: 10.1016/j.jvolgeores.2014.01.009

Aravena, Á, Cioni, R., de' Michieli Vitturi, M., and Neri, A. (2018). Conduit stability effects on intensity and steadiness of explosive eruptions. *Sci. Rep.* 8:4125. doi: 10.1038/s41598-018-22539-8

Aravena, Á, de' Michieli Vitturi, M., Cioni, R., and Neri, A. (2017). Stability of volcanic conduits during explosive eruptions. *J. Volcanol. Geotherm. Res.* 339, 52–62. doi: 10.1016/j.jvolgeores.2017.05.003

Barsotti, S., Andronico, D., Neri, A., Del Carlo, P., Baxter, P. J., Aspinall, W. P., et al. (2010). Quantitative assessment of volcanic ash hazards for health and infrastructure at Mt Etna (Italy) by numerical simulation. *J. Volcanol. Geotherm. Res.* 192, 85–96. doi: 10.1016/j.jvolgeores.2010.02.011

Behncke, B., Branca, S., Corsaro, R. A., De Beni, E., Miraglia, L., and Proietti, C. (2014). The 2011–2012 summit activity of Mount Etna: birth, growth and products of the new SE crater. *J. Volcanol. Geotherm. Res.* 270, 10–21. doi: 10.1016/j.jvolgeores.2013.11.012

Behncke, B., and Neri, M. (2019). *L'Etna Sbuffa Ed Emette Cenere: Nuova Eruzione o Attività di routine? Blog INGVvulcani, 19 Febbraio 2019.*

Available at: https://ingvvulcani.wordpress.com/2019/02/19/letna-sbuffa-ed-emette-cenere-nuova-eruzione-o-attivita-di-routine/ (accessed Feburary 19, 2019).

Bonaccorso, A. (2006). Explosive activity at Mt. Etna summit craters and source modeling by using high-precision continuous tilt. *J. Volcanol. Geotherm. Res.* 158, 221–234. doi: 10.1016/j.jvolgeores.2006.05.007

Bonaccorso, A., Cannata, A., Corsaro, R. A., Di Grazia, G., Gambino, S., Greco, F., et al. (2011). Multidisciplinary investigation on a lava fountain preceding a flank eruption: the 10 May 2008 Etna case, *Geochem. Geophys. Geosyst.* 12:Q07009. doi: 10.1029/2010GC003480

Cannata, A., Catania, A., Alparone, S., and Gresta, S. (2008). Volcanic tremor at Mt. Etna: inferences on magma dynamics during effusive and explosive activity. *J. Volcanol. Geotherm. Res.* 178, 19–31. doi: 10.1016/j.jvolgeores.2007.11.027

Cannata, A., Di Grazia, G., Giuffrida, M., Gresta, S., Palano, M., Sciotto, M., et al. (2018). Space-time evolution of magma storage and transfer at Mt. Etna volcano (Italy): the 2015-2016 reawakening of Voragine crater. *Geochem. Geophys. Geosyst.* 19, 471–495. doi: 10.1002/2017GC007296

Coltelli, M., Del Carlo, P., and Pompilio, M. (2000). Etna: eruptive activity in 1996. *Acta Vulcanol.* 1, 63–67.

Coltelli, M., Pompilio, M., Del Carlo, P., Calvari, S., Pannucci, S., and Scribano, V. (1998). Mt Etna – 1993–95 eruptive activity. *Acta Vulcanol.* 1, 141–148.

Corsaro, R. A., Andronico, D., Behncke, B., Branca, S., De Beni, E., Caltabiano, T., et al. (2017). Monitoring the December 2015 summit eruptions of Mt. Etna (Italy): implications on eruptive dynamics. *J. Volcanol. Geotherm. Res.* 341, 53–69. doi: 10.1016/j.jvolgeores.2017.04.018

Cristaldi, A., and Scollo, S. (2006). *Rapporto Sull'emissione Di Cenere all'Etna Nei Giorni 29 e 31 ottobre 2006*. Italy. INGV Internal Report No UFVG2006/128.

De Beni, E., Behncke, B., Branca, S., Nicolosi, I., Carluccio, R., D'Ajello Caracciolo, F., et al. (2015). The continuing story of Etna's new southeast crater (2012–2014): evolution and volume calculations based on field surveys and aerophotogrammetry. *J. Volcanol. Geotherm. Res.* 303, 175–186. doi: 10.1016/j.jvolgeores.2015.07.021

De Beni, E., Norini, G., and Polacci, M. (2006). *Aggiornamento Dell'attività Eruttiva (24 Novembre 2006, ore 13:00). Internal*. Available at: http://www.ct.ingv.it/Report/ (accessed November 24, 2006).

D'Oriano, C., Bertagnini, A., Cioni, R., and Pompilio, M. (2014). Identifying recycled ash in basaltic eruptions. *Sci. Rep.* 4:5851. doi: 10.1038/srep05851

Edwards, M. J., Pioli, L., Andronico, D., Scollo, S., Ferrari, F., and Cristaldi, A. (2018). Shallow factors controlling the explosivity of basaltic magmas: the 17–25 May 2016 eruption of Etna Volcano (Italy). *J. Volcanol. Geotherm. Res.* 357, 425–436. doi: 10.1016/j.jvolgeores.2018.05.015

Giuffrida, M., Viccaro, M., and Ottolini, L. (2018). Ultrafast syn-eruptive degassing and ascent trigger high-energy basic eruptions. *Sci. Rep.* 8:147. doi: 10.1038/s41598-017-18580-8

Harris, A. J. L., and Neri, M. (2002). Volumetric observations during paroxysmal eruptions at Mount Etna: pressurized drainage of a shallow chamber or pulsed supply? *J. Volcanol. Geotherm. Res.* 116, 79–95. doi: 10.1016/s0377-0273(02)00212-3

Horwell, C. J., Sargent, P., Andronico, D., Lo Castro, M. D., Tomatis, M., Hillman, S. E., et al. (2017). The iron-catalysed surface reactivity and health-pertinent physical characteristics of explosive volcanic ash from Mt. Etna, Italy. *J. Appl. Volcanol.* 6:12. doi: 10.1186/s13617-017-0063-8

Jaupart, C., and Vergniolle, S. (1988). Laboratory models of hawaiian and strombolian eruptions. *Nature* 331, 58–60. doi: 10.1038/331058a0

Jaupart, C., and Vergniolle, S. (1989). The generation and collapse of a foam layer at the roof of a basaltic magma chamber. *J. Fluid Mech.* 203, 347–380. doi: 10.1017/S0022112089001497

La Delfa, S., Patane, G., Clocchiatti, R., Joron, J. L., and Tanguy, J. C. (2001). Activity of Mount Etna preceding the february 1999 fissure eruption: inferred mechanism from seismological andgeochemical data. *J. Volcanol. Geotherm. Res.* 105, 121–139. doi: 10.1016/S0377-0273(00)00249-243

La Spina, A., Burton, M., Allard, P., Alparone, S., and Muré, F. (2015). Open-path FTIR spectroscopy of magma degassing processes during eight lava fountains on Mount Etna. *Earth Planet. Sci. Lett.* 413, 123–134. doi: 10.1016/j.epsl.2014.12.038

La Spina, G., Burton, M., de' Michieli Vitturi, M., and Arzilli, F. (2016). Role of syn-eruptive plagioclase disequilibrium crystallization in basaltic magma ascent dynamics. *Nat. Commun.* 7:13402. doi: 10.1038/ncomms13402

Neri, M. (2018). *L'eruzione Laterale Etnea Iniziata il 24 Dicembre 2018. Blog INGVvulcani*. Available at: https://ingvvulcani.wordpress.com/2018/12/25/leruzione-laterale-etnea-iniziata-il-24-dicembre-2018/ (accessed December 25, 2018).

Nicotra, E., and Viccaro, M. (2012). Transient uprise of gas and gas-rich magma batches fed the pulsating behaviour of the 2006 eruptive episodes at Mt. Etna volcano. *J. Volcanol. Geotherm. Res.* 227-228, 102–118. doi: 10.1016/j.jvolgeores.2012.03.004

Patrick, M. R., Harris, A. J. L., Ripepe, M., Dehn, J., Rothery, D. A., and Calvari, S. (2007). Strombolian explosive styles and source conditions: insights from thermal (FLIR) video. *Bull. Volcanol.* 69, 769–784. doi: 10.1007/s00445-006-0107-100

Pioli, L., Erlund, E., Johnson, E., Cashman, K., Wallace, P., Rosi, M., et al. (2008). Explosive dynamics of violent strombolian eruptions: the eruption of Parícutin Volcano 1943–1952 (Mexico). *Earth. Planet. Sci. Lett.* 271, 358–368. doi: 10.1016/j.epsl.2008.04.026

Polacci, M., Burton, M. R., La Spina, A., Murè, F., Favretto, S., and Zanini, F. (2009). The role of syn-eruptive vesiculation on explosive basaltic activity at Mt. Etna, Italy. *J. Volcanol. Geotherm. Res.* 179, 265–269. doi: 10.1016/j.jvolgeores.2008.11.026

Polacci, M., Corsaro, R. A., and Andronico, D. (2006). Coupled textural and compositional characterization of basaltic scoria: insights into the transition from strombolian to fire fountain activity at Mount Etna. Italy. *Geology* 34, 201–204. doi: 10.1130/G22318.1

Polacci, M., de' Michieli Vitturi, M., Arzilli, F., Burton, M. R., and Carr, B. (2017). From magma ascent to ash generation: investigating volcanic conduit processes by integrating experiments, numerical modeling, and observations. *Ann. Geophys.* 60:S0666. doi: 10.4401/ag-7449

Pompilio, M., Bertagnini, A., Del Carlo, P., and Di Roberto, A. (2017). Magma dynamics within a basaltic conduit revealed by textural and compositional features of erupted ash: the December 2015 Mt. Etna paroxysms. *Sci. Rep.* 7:4805. doi: 10.1038/s41598-017-05065-x

Poret, M., Corradini, S., Merucci, L., Costa, A., Andronico, D., Montopoli, M., et al. (2018a). Reconstructing volcanic plume evolution integrating satellite and ground-based data: application to the 23 November 2013 Etna eruption. *Atmos. Chem. Phys.* 18, 4695–4714. doi: 10.5194/acp-18-4695-2018

Poret, M., Costa, A., Andronico, D., Scollo, S., Gouhier, M., and Cristaldi, A. (2018b). Modeling eruption source parameters by integrating field, ground-based, and satellite-based measurements: the case of the 23 February 2013 Etna paroxysm. *J. Geophys. Res. Solid Earth* 123, 5427–5450. doi: 10.1029/2017JB015163

Romero, J. E., Vera, F., Polacci, M., Morgavi, D., Arzilli, F., Ayaz Alam, M., et al. (2018). Tephra from the 3 March 2015 sustained column related to explosive lava fountain activity at Volcán Villarrica (Chile). *Front. Earth Sci.* 6:98. doi: 10.3389/feart.2018.00098

Scollo, S., Del Carlo, P., and Coltelli, M. (2007). Tephra fallout of 2001 Etna flank eruption: analysis of the deposit and plume dispersion. *J. Volcanol. Geotherm. Res.* 160, 147–164. doi: 10.1016/j.jvolgeores.2006.09.007

Scollo, S., Prestifilippo, M., Pecora, E., Corradini, S., Merucci, L., Spata, G., et al. (2014). Eruption column height 25 estimation of the 2011-2013 Etna lava fountains. *Ann. Geophys.* 57:S0214. doi: 10.4401/ag-6396

Taddeucci, J., Pompilio, M., and Scarlato, P. (2002). Monitoring the explosive activity of the july –august 2001 eruption of Mt. Etna (Italy) by ash characterization. *Geophys. Res. Lett.* 29, 1–4. doi: 10.1029/2001GL014372

Taddeucci, J., Pompilio, M., and Scarlato, P. (2004). Conduit processes during the july–august explosive activity of Mt. Etna (Italy): inferences from glass

chemistry and crystal size distribution of ash particles. *J. Volcanol. Geotherm. Res.* 137, 33–54. doi: 10.1016/j.jvolgeores.2004.05.011

Vergniolle, S., and Ripepe, M. (2008). From strombolian explosions to fire fountains at Etna Volcano (Italy): what do we learn from acoustic measurements? *Geol. Soc. Lond. Spec. Publ.* 307: 103–124.

Villani, M. G., Mona, L., Maurizi, A., Pappalardo, G., Tiesi, A., Pandolfi, M., et al. (2006). Transport of volcanic aerosol in the troposphere: the case study of the 2002 Etna plume. *J. Geophys. Res.* 111:D21102. doi: 10.1029/2006JD007126

Vulpiani, G., Ripepe, M., and Valade, S. (2016). Mass discharge rate retrieval combining weather radar and thermal camera observations. *J. Geophys. Res. Solid Earth.* 121, 5679–5695. doi: 10.1002/2016jb013191

Conflict of Interest Statement: The authors declare that the research was conducted in the absence of any commercial or financial relationships that could be construed as a potential conflict of interest.

The reviewer MV declared a shared affiliation, with no collaboration, with the authors, DA, AC, to the handling Editor at the time of review.